A Mathematical Model of a Biosensor

N. Botkin, M. Schlensog, M. Tewes and V. Turova

center of advanced european studies and research,
Friedensplatz 16, 53111 Bonn, Germany, turova@caesar.de

ABSTRACT

A mathematical model of a biosensor is considered. The biosensor is supposed to be used for the measurement of small amounts of certain substances in liquids. The device works as follows: acoustic shear waves are excited due to an alternate voltage applied to electrodes deposited on a quartz crystal substrate; the waves are transmitted into a thin isotropic guiding layer that contacts a liquid containing molecules to be detected; this ligand adheres to a specific receptor (aptamer) immobilized on the surface of the guiding layer; arising mass loading causes a phase shift in the electric signal to be measured by the sensor. The mathematical model represents a composite structure consisting of three coupled layers: two solid layers with different elastic and electric properties and a liquid layer treated as a compressible viscous fluid. The full coupling between deformations and the electric field is assumed. The technique developed in [3] is used for the model statement. The numerical realization of the model is based on the finite element method. Computer simulations are in a good agreement with physical experiments.

Keywords: linear electro-elasticity, multi-layer structure, fluid-structure interaction, finite elements method.

1 INTRODUCTION

One of very promising applications of acoustic wave sensors is the measurement of small amounts of chemical and biological substances in liquids (see e.g. [2], [4]). A high sensitivity regarding mass loading is expected to be achieved due to the usage of shear waves because of their low interaction with the contacting fluid. Figure 1 presents a schematic picture of the biosensor. A thin film (isotropic guiding layer) is deposited on a substrate made of a quartz crystal. The input and output interdigital transducers (IDTs) are located between the substrate and film. To obtain purely shear polarized modes (the displacements along the axis x_2), the direction of the wave propagation is chosen to be orthogonal to the crystall's X-axis. The choice of the film and substrate materials must provide that the wave velocity in the film is less than the one in the substrate so that the waves will be transferred into the film.

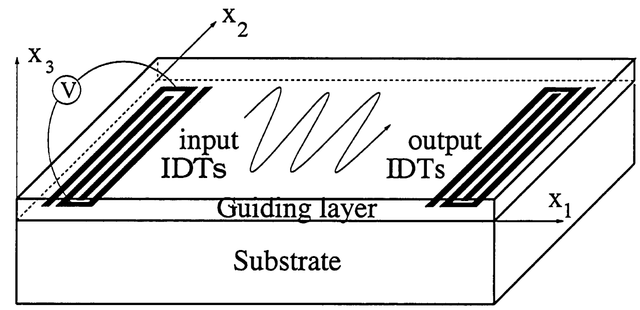

Figure 1: A draft of a biosensor

2 TWO-DIMENSIONAL MODEL

The following notation will be used: u_1, u_2 and u_3 are the displacements in the x_1-, x_2- and x_3-directions, φ is the electric potential, v_1, v_2 and v_3 are the velocity components, p is the pressure caused by acoustic waves, ϱ is the density of the fluid, $u_{i,j}$ and $\varphi_{,i}$ are the partial derivatives $\partial u_i/\partial x_j$ and $\partial\varphi/\partial x_i$, respectively. Bold letters indicate vectors. Summation over repeated indices is assumed.

We suppose that u_i, φ, v_i, p and ϱ do not depend on x_2, that is $u_i = u_i(x_1, x_3)$, $\varphi = \varphi(x_1, x_3)$, $v_i = v_i(x_1, x_3)$, $p = p(x_1, x_3)$ and $\varrho = \varrho(x_1, x_3)$. Figure 2 presents a schematic picture of the three-layer structure corresponding to the two-dimensional concept. The regions occupied by the isotropic layer and the substrate are labeled with S_U and S_L. The fluid layer is labeled with S_F. The input IDTs of two alternated groups are indicated as S_1 and S_2, the output IDTs as S_3 and S_4.

2.1 Electro-elasticity Equations

We consider linear material laws (see [7]):

$$\sigma^{(1)ij} = C^{(1)ijkl}\varepsilon_{kl} \quad (1)$$

$$\sigma^{(2)ij} = C^{(2)ijkl}\varepsilon_{kl} - e^{kij}E_k = \tilde{\sigma}^{(2)ij} - e^{kij}\varphi_{,k} \quad (2)$$

$$D^i = \epsilon^{ij}E_j + e^{ikl}\varepsilon_{kl} = \epsilon^{ij}\varphi_{,j} + e^{ikl}\varepsilon_{kl}. \quad (3)$$

Here $\sigma^{(1)ij}$ and $\sigma^{(2)ij}$ are the stress tensors, $C^{(1)ijkl}$ and $C^{(2)ijkl}$ are the elastic stiffness tensors for the isotropic

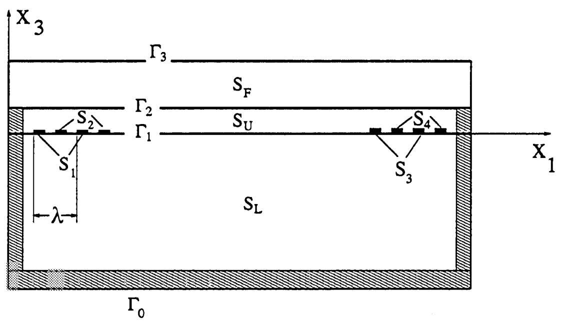

Figure 2: Two-dimensional model

and piezoelectric materials, respectively; $\varepsilon_{ij} = \frac{1}{2}(u_{i,j} + u_{j,i})$ is the strain tensor, ϵ^{ij} and e^{kij} are material dielectric and piezoelectric stress tensors, $E_k = \varphi_{,k}$ are components of the electric field. The energy density for the isotropic layer is given by the formula (see [5]):

$$F^{(1)} = \frac{E}{2(1+\varsigma)}\left(\varepsilon_{ij}^2 + \frac{\varsigma}{1-2\varsigma}(\varepsilon_{ii})^2\right),$$

where E is the Young's modulus and ς is the Poisson ratio. For the piezoelectric layer, the energy density is

$$F^{(2)} = \frac{1}{2}(\sigma^{(2)ij}\varepsilon_{ij} - D^i E_i).$$

Here, D^i are components of the dielectric displacement. Using (2) and (3), we obtain

$$F^{(2)} = \frac{1}{2}(\widetilde{\sigma}^{(2)ij}\varepsilon_{ij} - 2e^{kij}\varepsilon_{ij}\varphi_{,k} - \epsilon^{ij}\varphi_{,i}\varphi_{,j}).$$

To take into account effects caused by the massiveness of the electrodes, we consider the energy density for the electrodes

$$F^{(3)} = \frac{E_e}{2(1+\varsigma_e)}\left(\varepsilon_{ij}^2 + \frac{\varsigma_e}{1-2\varsigma_e}(\varepsilon_{ii})^2\right),$$

where E_e is the Young's modulus and ς_e is the Poisson ratio for the electrodes material.

The total energy is obtained through the integration of the energy densities over the volumes $V^{(1)}$, $V^{(2)}$ and $V^{(3)}$ of the guiding layer, the substate and the electrodes, respectively:

$$\mathcal{F} = \iiint\limits_{V^{(1)}} F^{(1)}dv + \iiint\limits_{V^{(2)}} F^{(2)}dv + \iiint\limits_{V^{(3)}} F^{(3)}dv.$$

We assume that $F^{(3)}$ does not depend on x_3, since the thickness h_e of the electrodes is much less than those for the guiding layer and substrate. Besides, using that $F^{(1)}$, $F^{(2)}$ and $F^{(3)}$ do not depend on x_2, we obtain

$$\mathcal{F} = b\Big(\iint\limits_{S_U} F^{(1)}ds + \iint\limits_{S_L} F^{(2)}ds + h_e\int\limits_S F^{(3)}dx_1\Big) =$$

$$b\left(\frac{E}{2(1+\varsigma)}\iint\limits_{S_U}(\varepsilon_{ij}^{(1)2} + \frac{2\varsigma}{1-2\varsigma}(\varepsilon_{ii}^{(1)})^2)dx_1dx_3 + \right.$$

$$\frac{1}{2}\iint\limits_{S_L}(\widetilde{\sigma}^{(2)ij}\varepsilon_{ij}^{(2)} - 2e^{kij}\varepsilon_{ij}^{(2)}\varphi_{,k} - \epsilon^{ij}\varphi_{,i}\varphi_{,j})dx_1dx_3 +$$

$$\left.\frac{E_e h_e}{2(1+\varsigma_e)}\int\limits_S(\varepsilon_{ij}^{(1)2} + \frac{2\varsigma_e}{1-2\varsigma_e}(\varepsilon_{ii}^{(1)})^2)dx_1\right),$$

where $S = \cup_{i=\overline{1,4}}S_i$ is a one-dimensional region occupied by the electrodes and b is the x_2-size of the biosensor.

To obtain differential equations describing the oscillation of the two-layer structure, we compute the variation $\delta\mathcal{F}$ of the total energy with respect to the vector $\boldsymbol{u} = (u_1, u_2, u_3)$ and the electric potential φ. The variational principle reads

$$\iint\limits_{S_U}\rho^{(1)}u_{i\,tt}\delta u_i dx_1dx_3 + \iint\limits_{S_L}\rho^{(2)}u_{i\,tt}\delta u_i dx_1dx_3 +$$

$$h_e\int\limits_S \rho_e u_{i\,tt}\delta u_i dx_1 + \delta\mathcal{F}/b = 0.$$

The first, second and third terms express the work of inertia forces. Symbols $\rho^{(1)}$, $\rho^{(2)}$ and ρ_e denote the densities of the guiding layer, substrate and electrode materials, respectively. Using that $u_{1,2} = u_{2,2} = u_{3,2} = 0$ and, therefore, $\delta u_{1,2} = \delta u_{2,2} = \delta u_{3,2} = 0$, we obtain

$$\delta\mathcal{F}/b = \frac{E}{2(1+\varsigma)}\iint\limits_{S_U}((u_{k,m}+u_{m,k})\delta u_{k,m} + u_{2,k}\delta u_{2,k} +$$

$$\frac{2\varsigma}{1-2\varsigma}u_{m,m}\delta u_{m,m})dx_1dx_3 + \iint\limits_{S_L}(\widetilde{\sigma}^{(2)im}\delta u_{i,m} -$$

$$e^{kim}\varphi_{,k}\delta u_{i,m} - e^{kim}u_{i,m}\delta\varphi_{,k} - \epsilon^{km}\varphi_{,k}\delta\varphi_{,m})dx_1dx_3 +$$

$$\frac{E_e h_e}{2(1+\varsigma_e)}\int\limits_S((u_{k,m}+u_{m,k})\delta u_{k,m} + u_{2,k}\delta u_{2,k} +$$

$$\frac{2\varsigma_e}{1-2\varsigma_e}u_{m,m}\delta u_{m,m})dx_1dx_3.$$

Here, i runs from 1 to 3 but k and m assume the values 1 and 3. Substituting the test functions ψ_1, ψ_2, ψ_3 and η instead of variations $\delta u_1, \delta u_2, \delta u_3$ and $\delta\varphi$, we obtain a week formulation of the problem:

$$\iint\limits_{S_U}\rho^{(1)}u_{i,tt}\psi_i dx_1dx_3 + \iint\limits_{S_L}\rho^{(2)}u_{i,tt}\psi_i dx_1dx_3 +$$

$$h_e\int\limits_S\rho^{(1)}u_{i,tt}\psi_i dx_1 + \frac{E}{2(1+\varsigma)}\iint\limits_{S_U}((u_{k,m}+u_{m,k})\psi_{k,m}$$

$$+ u_{2,k}\psi_{2,k} + \frac{2\varsigma}{1-2\varsigma} u_{m,m}\psi_{m,m}) dx_1 dx_3 + \quad (4)$$

$$\int\int_{S_L} (\widetilde{\sigma}^{(2)im}\psi_{i,m} - e^{kim}\varphi_{,k}\psi_{i,m} - e^{kim}u_{i,m}\eta_{,k} -$$

$$\epsilon^{km}\varphi_{,k}\eta_{,m}) dx_1 dx_3 + \frac{E_e h_e}{2(1+\varsigma_e)} \int_S ((u_{k,m} + u_{m,k})\psi_{k,m}$$

$$+ u_{2,k}\psi_{2,k} + \frac{2\varsigma_e}{1-2\varsigma_e} u_{m,m}\psi_{m,m}) dx_1 = 0.$$

To avoid reflections on the boundaries of the device, a damping on the boundaries is introduced as follows: the term $-\lambda \iint_{\mathcal{H}} (u_{1t,1}\psi_{1,1} + u_{2t,2}\psi_{2,2} + u_{3t,3}\psi_{3,3}) dx_1 dx_3$, where $\mathcal{H}$ is the shaded region in Figure 2, is added on the left-hand-side of (4).

If we do not take into account the massiveness of the electrodes, the integrals over S vanish and the equations can be written in the classical form:

$$\rho^{(1)} u_{i\,tt} - \frac{\partial}{\partial x_m}\sigma^{(1)im} = 0, \quad x \in S_U$$

$$\rho^{(2)} u_{i\,tt} - \frac{\partial}{\partial x_m}\sigma^{(2)im} + e^{kim}\frac{\partial^2 \varphi}{\partial x_m \partial x_k} = 0, \quad x \in S_L$$

$$\epsilon^{im}\frac{\partial^2 \varphi}{\partial x_i \partial x_m} + e^{kim}\frac{\partial^2 u_i}{\partial x_k \partial x_m} = 0, \quad x \in S_L.$$

2.2 Equations for the Fluid Layer

In the fluid layer, the following Stokes equation

$$\rho v_t - \nu \Delta v + \nabla p = 0, \quad x \in S_F \quad (5)$$

together with the continuity equation:

$$\varrho_t + \varrho \,\mathrm{div} v = 0, \; x \in S_F, \quad (6)$$

and the substitutive equation

$$\varrho = \varrho_0 + \frac{\partial \varrho}{\partial p}\Big|_{\varepsilon} p$$

are considered. Here, ν is the viscosity coefficient of the fluid.

2.3 Interface and Boundary Conditions

Let n_j be the components of the normal vector $\boldsymbol{n}$ to a region. The following interface and boundary conditions are posed:

a) Absence of forces on Γ_0 : $\sigma^{(1)ij} n_j = 0, \; \sigma^{(2)ij} n_j = 0,$

b) Continuity of the displacement vector $\boldsymbol{u}$ and equilibrium of the pressures on Γ_1 : $\sigma^{(1)ij} n_j = \sigma^{(2)ij} n_j,$

c) Dirichlet conditions for the electric potential:

$\varphi|_{S_1} = 0, \; \varphi|_{S_2} = V(t), \; \varphi|_{S_3} = C(t), \; \varphi|_{S_4} = 0,$

where $V(t)$ is a given exciting voltage and $C(t)$ is the output voltage to be determined from the equations,

d) Neuman condition for the electric potential:

$\frac{\partial \varphi}{\partial n} = 0$ for (x_1, x_3) outside IDTs.

e) Equilibrium of the pressures on Γ_2:

$\nu \frac{\partial v_i}{\partial n} - p_i = \sigma^{(1)ij}(u) n_j,$

$\boldsymbol{n}$ is the outer normal to the rigid body,

f) Continuity of the velocity on Γ_2: $\frac{\partial \boldsymbol{u}}{\partial t} = \boldsymbol{v},$

g) No-slip condition on Γ_3 : $\boldsymbol{v} = 0.$

Note that the condition f) is the most difficult to fulfil. The following scheme from [6] is used. We do the following variable transformation in the electro-elasticity equations: $\boldsymbol{u} = \int_0^t \hat{\boldsymbol{v}}\, d\tau$, where $\hat{\boldsymbol{v}}$ is a new variable. Then the condition f) is equivalent to the condition $\hat{v} = v$ on Γ_2. It is proven in [6] that the obtained coupled system has a unique solution.

2.4 Steady-state Solutions

Let ω denote the operating frequency of the IDTs. Taking $V(t) = A\sin\omega t + B\cos\omega t$ and substituting the ansatz

$$\begin{aligned} u_i(x_1,x_3,t) &= r_i(x_1,x_3)\sin\omega t + q_i(x_1,x_3)\cos\omega t,\\ \varphi(x_1,x_3,t) &= \varphi_1(x_1,x_3)\sin\omega t + \varphi_2(x_1,x_3)\cos\omega t,\\ v_i(x_1,x_3,t) &= g_i(x_1,x_3)\sin\omega t + s_i(x_1,x_3)\cos\omega t,\\ p(x_1,x_3,t) &= p_1(x_1,x_3)\sin\omega t + p_2(x_1,x_3)\cos\omega t, \end{aligned} \quad (7)$$

for $i = 1,2,3$ into the equations (4)–(6) and the boundary conditions a)–g) yield equations and boundary conditions for the time-independent functions r_i, q_i, φ_1, φ_2, g_i, s_i, p_1 and p_2. These equations are similar to (4).

We refer to the time-independent functions r_i, q_i, g_i, s_i, f_1, f_2, p_1 and p_2 as the steady-state solutions.

Program codes for the computation of both time-dependent and steady-state solutions were developed.

3 NUMERICAL REALIZATION

The above model is realized on the base of the finite element program FeliCs developed on the chair of Applied Mathematics and Mechanics at the Technical University of Munich. Triangle linear finite elements are used. A parallelized version of the program SPOOLS (see [1]) for solving systems of linear algebraic equations is used. A MAPLE-program for automatic derivation of the model equations is developed. This program computes the total energy and its variations in the symbolic form and derives the model equations in a form appropriate for the input of FeliCs. Using this program, one can transform the coordinate system and obtain equations for various crystal cuts.

4 SIMULATION RESULTS

The simulations are done for the following material and device parameters. The guiding layer is made of SiO_2 with $\rho^{(1)} = 2180\,kgm^{-3}$, $\sigma = 0.17$ and $E = 72\,GPa$, the electrodes are made of gold with $\rho^{(1)} = 19300\,kgm^{-3}$, $\sigma = 0.44$ and $E = 78\,GPa$. For the substrate, CT-cut of a quartz crystal is used. The fluid is water ($\nu = 0.001\,\frac{kg}{m\,s}$). Figures 3–5 show steady-state solutions in the substrate, guiding layer and fluid, respectively. The vertical axis in Figures 3 and 4 measures the x_2-displacements (function r_2 in (7)). In Figure 5, the vertical axis measures the x_2-velocity in the fluid (function g_2 in (7)). The computation is done for three pairs of electrodes. The periodicity λ of the sensor is $40\,\mu m$, the operating frequency is 81 MHz. We obtain strong attenuation of shear waves in the substrate and good wave transfer into the guiding layer. The penetration depth of shear waves into the fluid is in the range of one wave length.

Simulations for a real sensor with 50 pairs of electrodes are also done. The computed value of the resonance frequency is in a good agreement with the value obtained from the measurement. High sensitivity of the model with respect to small mass loadings is also proved. In Figure 6, the graph of the phase shift for the output signal versus the thickness of the adhering molecule film which is modeled as a gold layer between the input and output IDTs is shown.

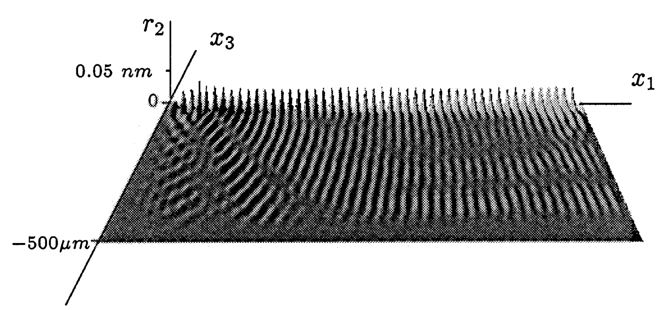

Figure 3: Shear waves in the substrate

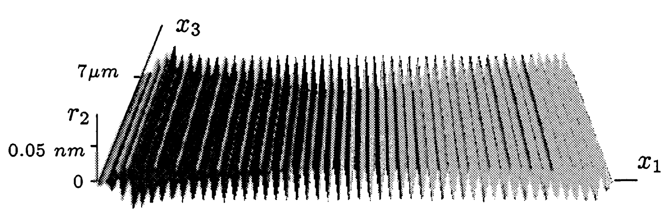

Figure 4: Shear waves in the guiding layer

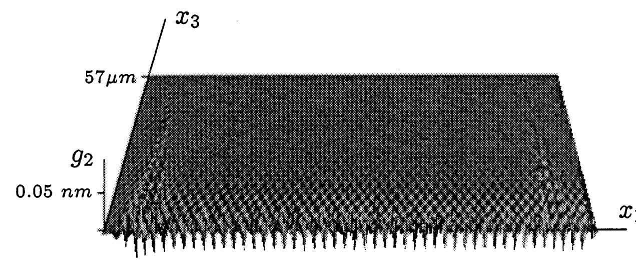

Figure 5: x_2- velocity in the fluid

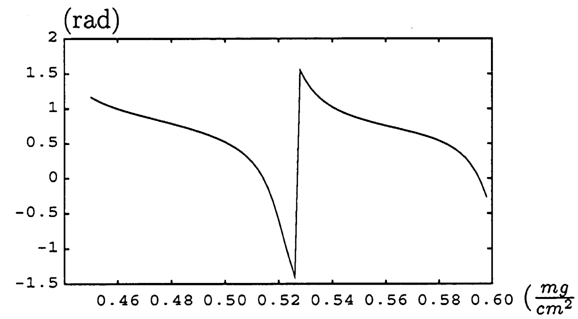

Figure 6: Phase shift for different mass loadings

REFERENCES

[1] *C. Ashcraft and R. Grimes, SPOOLES: an object-oriented sparse matrix library, 9th SIAM Conference on Parallel Processing for Scientific Computing, March 1999, San Antonio, Texas.*

[2] *H. Drobe, A. Leidl, M. Rost and I. Ruge, Acoustic Sensors Based on Surface-localized HPSWs for Measurements in Liquids, Sensors and Actuators, 4, 141–148, 1993.*

[3] *K.-H. Hoffmann and N.D. Botkin, Oscillations of Nonlinear Thin Plates Excited by Piezoelectric Patches, ZAMM, 78, 1998, 495-503.*

[4] *G. Kovacs, M.J. Vellekoop, R. Haueis, G.W. Lubking and A. Venema, A Love Wave Sensor for (Bio)chemical Sensing in Liquids, Sensors and Actuators A, 43, 38–43, 1994.*

[5] *L.D. Landau and E.M. Lifschitz, Elastizitätstheorie, Akademie–Verlag, Berlin, 1975.*

[6] *J.L. Lions, Quelques Methodes de Resolution des Problemes aux Limites non Lineaires, Dunod Gauthier-Villars, Paris, 1969.*

[7] *J. Zelenka, Piezoelectric Resonators and their Applications, Studies in Electrical and Electronic Engineering, 24, Elsevier 1986.*